

*Scientific Category: Immunobiology*

*e-Blood*

**Manipulating leukocyte interactions in vivo  
through optogenetic chemokine release**

Milka Sarris<sup>1,2,3</sup>, Romain Olekhnovitch<sup>1,2,4</sup>, Philippe Bousso<sup>1,2</sup>

<sup>1</sup>Institut Pasteur, Dynamics of Immune Responses Unit, 75015 Paris, France.

<sup>2</sup>INSERM U668, rue du Dr Roux, 75015 Paris, France.

<sup>3</sup>University of Cambridge, Department of Physiology, Development and Neuroscience,  
Downing site CB2 3DY, Cambridge, UK

<sup>4</sup>University Paris Diderot, Sorbonne Paris Cité, Cellule Pasteur, rue du Dr Roux, 75015  
Paris, France.

Correspondence:

Milka Sarris ([ms543@cam.ac.uk](mailto:ms543@cam.ac.uk)) and Philippe Bousso ([philippe.bousso@pasteur.fr](mailto:philippe.bousso@pasteur.fr))

Running title: Optogenetic control of leukocyte communication

## **Key points**

- We report a method to optogenetically control the release of soluble mediators such as chemokines and influence immune cell migration.
- This approach is applicable to a variety of secreted ligands and can facilitate dynamic, in situ studies of immune cell communication

## **Abstract**

**Light-mediated release of signalling ligands, such as chemoattractants, growth factors and cytokines is an attractive strategy for investigation and therapeutic targeting of leukocyte communication and immune responses. We introduce a versatile optogenetic method to control ligand secretion, combining UV-conditioned ER-to-Golgi trafficking and a furin-processing step. As proof of principle, we achieved light-triggered chemokine secretion and demonstrated that a brief pulse of chemokine release can mediate a rapid flux of leukocyte contacts with target cells in vitro and in vivo. This approach opens new possibilities for dynamic investigation of leukocyte communication in vivo and may confer the potential to control the local release of soluble mediators in the context of immune cell therapies.**

## Introduction

The secretion and graded distribution of diffusible mediators represents a major mode of cell-cell communication that is essential for immune responses. However, we still have a poor understanding of how soluble signalling mediators propagate and act *in vivo*. What is their temporal and spatial range of action? How much ligand needs to be produced and by how many cells for a biological effect *in vivo*? How do leukocytes respond to dynamic signal inputs in tissue? The ability to spatiotemporally manipulate production of signalling ligands *in situ* would provide a means to answer several fundamental questions of this nature and to locally control immune cell functions during cell therapy, yet has so far remained a technological challenge.

One experimental development in this direction is the chemical synthesis of caged signalling ligands<sup>1</sup>. For example administration of chemically-produced caged chemokines was shown to control cell positioning of leukocytes *in vivo*<sup>1</sup>. A second approach, by means of optogenetics, is to generate chimaeras of G-protein coupled receptors, such as chemokine receptors, with rhodopsin, which has allowed manipulation of leukocyte migration by light<sup>2</sup>. However, these approaches bypass natural ligand propagation or recognition. In addition, rhodopsin chimaeras are not applicable to non-GPCR receptor signaling. Light-mediated control of protein activity and distribution by means of other optogenetic modules, such as CRY2, LOV or UVR8, offer further possibilities to manipulate cell signaling<sup>3</sup>. Optogenetic control of ligand release *in vivo* would represent a very attractive strategy to interrogate basic mechanisms of intercellular communication by diffusible proteins. Such an approach would offer new possibilities over existing methods: i) use of a cellular source for production of the soluble mediator, allowing dynamic studies of intercellular communication, ii) targeted expression in

specific cell types or tissues, iii) minimised intervention with physiological ligand propagation and recognition mechanisms, iv) absence of added exogenous factors, a potential a source of complication for in vivo studies and applications. Although strategies for transcriptional control of ligand production have been described (ranging from optogenetically-controlled<sup>4,5</sup>, pharmacologically-controlled<sup>6</sup> or temperature-controlled transcription<sup>7</sup>), such approaches have limited dynamic range, since ligand would require a considerable amount of time to be secreted by the cells. Strategies to trigger ligand secretion are more rapid but have so far been based on chemical-genetic induction<sup>8,9</sup>.

Here we present a first optogenetic method to deliver rapid pulsatile ligand secretion and manipulate cell communication by light in situ.

## Methods

### Animals

C57BL/6 transgenic mice expressing GFP under the control of the human ubiquitin C promoter<sup>20</sup> in wild type or Rag2<sup>-/-</sup> background were used for the transwell chemotaxis experiments. BALB/c LysM-EGFP<sup>15</sup> mice were used for in vivo interaction assays and mTomato mice<sup>21</sup> were used for in vitro interaction assays. All mice were bred under specific pathogen-free conditions at Institut Pasteur. Mouse experiments were performed in accordance to the guidelines of Institut Pasteur for animal care and use. Tg(*mpx:Lifeact-Ruby*) and Tg(*lyz:DsRed*)<sup>nz50</sup> zebrafish were bred and handled in the University of Cambridge according to institutional and UK guidelines (Home Office Licence number: 70/8255).

### Plasmids

sec-mCherry (as in<sup>13</sup>), murine Cxcl2 or zebrafish Cxcl8 were designed to be at the N-terminal end, followed by a linker sequence, a furin cleavage site (amino acid sequence SARNRQKR), VSVG-ts045, YFP and 2 UVR8 repeats. Inserts were synthesized by GeneWiz and cloned using BamHI and Hind III into a retroviral and mammalian expression vector pMSCV. Wild type Cxcl2 was synthesized alongside and cloned using BamHI and Hind III into pMSCV. Zebrafish Cxcl8 was subcloned into the same backbone vector pMSCV-YFP-2xUVR8.

### Cell culture and transfection

HEK293T cells were cultured in DMEM (Invitrogen) containing 10% FBS (Hyclone) and were transfected with plasmids using Lipofectamine 2000 (Invitrogen). With the

exception of zebrafish cell interaction experiments, HEK293T cells were used 16-24h post transfection.

### **Imaging of mCherry-UVR8 redistribution**

HEK293T cells were transfected in imaging dishes (Ibidi) and 16-18h later the cells were exposed to UVB light (3-24 mJ) using a X97 UVB-BB (280-320 nm) lamp (DAAVLIN). Immediately after, the cells were imaged in an Olympus Confocal System (FV1000MPE) using a 40x/0.95 NA objective or a Leica SP8 confocal using a 20x/0.75 NA objective. mCherry was excited using a 560 nm laser and YFP was excited using a 488 nm laser. Thin z-stacks of about 10  $\mu\text{m}$  thickness with a spacing of approximately 2  $\mu\text{m}$  were acquired. Maximum intensity projection of confocal stacks was performed using ImageJ.

### **Western blotting**

HEK293T cells were transfected and 16-18h later, medium was replaced with fresh medium. Immediately after, cells were exposed to UVB light (6-24 mJ), using a X97 UVB-BB (280-320 nm) lamp (DAAVLIN), and then incubated for 2-3h at 32°C. Conditioned medium was then concentrated 50-100 fold using Vivaspin columns (Sartorius) of appropriate molecular weight cut-off (as an indication, a blot lane would typically be loaded with supernatant corresponding to  $\frac{1}{4}$  of a confluent 10 cm dish of HEK293T cells). Cell lysates were prepared in RIPA buffer (Invitrogen) and EDTA-free protease inhibitors (Roche). Samples were run on a 10-12% SDS-PAGE (Nupage) and blotted using the Nupage iBlot system. For detection of mCherry, anti-DsRed (Clontech) was used at 1:1000 and for detection of Cxcl2 we used anti-Cxcl2 (R&D systems) at a dilution of 1:300-1000. Revelation was performed using a Supersignal West Femto Maximum Sensitivity Substrate kit (Life Technologies) or ECL Prime Western Blotting

Detection kit (GE Healthcare). For the time-course of Cxcl2 secretion we collected cell supernatants in 30 min intervals after photoactivation, washing the cells in between collection time points, to assess new chemokine secretion. For this experiment, 30 sec exposure to a UVB source of wavelength 312 nm was used (EB280C supported by a SE-140 stage; UVMAN). For calibration of protein amount, recombinant Cxcl2 (R&D systems) of known concentration was loaded on the blot. Lane densitometry was performed in Fiji.

### **In vitro transwell chemotaxis assay**

HEK293T cells 1 day post-transfection with UVR8-YFP constructs were briefly washed, without disturbing the cell monolayer, and replenished with fresh medium (serum-free and phenol red-free RPMI). Cells were exposed to UVB (9 mJ), using an X97 UVB-BB (280-320 nm) lamp (DAAVLIN), and incubated at 32°C for 3-4h. Supernatants were concentrated (about 12-fold) and stored at -20°C for use the following day. GFP<sup>+</sup> neutrophils were prepared from bone marrow extracted from Rag<sup>-/-</sup>xUbiGFP mice, using the Miltenyi Neutrophil isolation kit (Miltenyi, negative selection kit). Single cell suspensions were made in RPMI/0.5% BSA (Calbiochem)/10 mM HEPES (Invitrogen) at a density of 1-1.3x10<sup>6</sup> cells/ml. Chemotaxis was assessed in a 96-well HTS Transwell system (Corning). 240 µl of culture supernatant or RPMI medium were added to the bottom chamber (each well would typically be loaded with supernatant corresponding to ½ of a 10 cm dish of HEK293T cells). In some cases supernatants were pre-incubated in anti-Cxcl2 (2 µg/ml final concentration, R&D systems) for 15-30 minutes on ice and then placed in the bottom chamber. 75 µl of neutrophil suspensions were placed in the upper chamber. After incubation for 3h at 37°C, cells in the bottom chamber were harvested and the number of GFP<sup>+</sup> cells was assessed by FACS analysis (FACS Canto, BD). The results

were normalized to Calibrite beads (BD) that had been added to each cell sample just before harvest, to ensure independence from volume and FACS fluctuations.

### **In vitro cell interaction assay**

HEK293T cells were seeded in 35mm imaging dishes (Ibidi) coated with poly-L-lysine (Sigma) and transfected in these dishes 1 day post-seeding. Neutrophils were purified from bone marrow extracted from mTomato mice<sup>21</sup>, using the Miltenyi Neutrophil isolation kit (Miltenyi, negative selection kit). Purity of the cell preparation was assessed via FACS and staining for the markers Ly6G and CD11b. Fresh neutrophils were re-suspended in imaging medium (RPMI phenol-red free / 10% FBS/ 10mM HEPES) and seeded on to HEK293T cells that had been transfected the previous day in imaging plates. Neutrophils were allowed to settle for a few minutes and then the culture was exposed to UVB light (doses ranging from 6-24 mJ), using a X97 UVB-BB (280-320 nm) lamp (DAAVLIN). As soon as possible after UV-exposure, plates were imaged under epifluorescence using a DMI 6000B inverted microscope (Leica microsystems) equipped with an environmental chamber for temperature, humidity, and 5% CO<sub>2</sub> (PECON), with a 20x/0.75 NA (Olympus) or 10x/0.45 NA (Nikon) dry objectives and a CoolSNAP HQ2 Roper camera (Photometrics, Tucson, AZ). Time lapse movies with an interval of 2 min were acquired in a multi-plex fashion. Temperature was maintained at 34-35 °C. Movies were processed in Imaris (Bitplane) and ImageJ.

### **Cell interaction assay in mouse tissue**

BALB/c LysM-EGFP mice were anesthetized, and the dorsal dermis of the ear was surgically exposed. Transfected HEK293T cells were seeded on the exposed dermis during 1 h. The ear was then rinsed several times with PBS and prepared for microscopy.



A quartz coverslip (Ted Pella Inc) was placed onto the ear and covered with deionized water to immerge a 25x/1.05 NA objective (Olympus). Two-photon imaging was performed using a DM6000 upright microscope equipped with a SP5 confocal head (Leica Microsystems, Wetzlar, Germany) and a Chamaeleon Ultra Ti:Sapphire laser (Coherent, Santa Clara, CA) tuned at 920 nm. Emitted fluorescence was passed to non-descanned detectors through dichroic mirrors. Typically, images from 15-20 z planes spaced 5  $\mu\text{m}$  were collected every 3 minutes. For UVR8 photoactivation, the ear dermis was exposed for 120 sec to a UVB source (310nm LED, Thorlabs) from a distance of 3 cm.

#### **Cell interaction assay in zebrafish**

HEK293T cells were transfected with a mock plasmid (pCAG-GFP) or Cxcl8-YFP-2xUVR8 plasmid and 5 hours later were implanted into *Tg(mpx:Lifeact-Ruby)*<sup>16</sup> or *Tg(lyz:DsRed)*<sup>nz50</sup> transgenic zebrafish embryos at 48 hpf as previously described<sup>13</sup>. Larvae were kept overnight at 34°C in E3 medium (5 mM NaCl, 0.15 mM KCl, 0.33 mM CaCl<sub>2</sub>, 0.33 mM mgSO<sub>4</sub>, methylene blue and 1-phenyl-2-thiourea). 18-24 hours post transplantation larvae were mounted in 1% low melting point agarose in 35mm dishes topped with E3 medium (without methylene blue) supplemented with 0.16 mg/ml tricaine (Sigma). Time-lapse confocal stacks (of between 35-50 slices spaced by 2  $\mu\text{m}$ ) were acquired with an interval of 15-30 sec on an upright Nikon E1000 microscope, using 40x/0.80NA water objective coupled to a Yokogawa CSU10 spinning disc confocal scanner unit and illuminated using a Spectral Applied Research LMM5 laser module (491 nm for YFP excitation; 561 nm for Ruby/DsRed) or on a Perkin Elmer Spinning Disk UltraVIEW ERS, Olympus IX81 inverted spinning disk confocal microscope, using a 20x/0.45 NA oil objective, 488nm for YFP excitation and 561nm for Ruby/DsRed.

Images were captured using Volocity software. Imaging was conducted within a custom-built heated chamber (for the upright scope) or a heated stage (for the inverted scope) and temperature was maintained at 32-35 °C. For UVR8 photoactivation the mounted larvae were exposed for 60 sec to a UVB source (312 nm; EB280C supported by a SE-140 stage; UVMAN) from a distance of 7 cm (power equivalent to 0.3 mW/cm<sup>2</sup> according to reference 10). When using an inverted scope, embryos were mounted on a quartz coverslip for maximum UV transmission. When using an upright scope, UV illumination was performed directly above the agarose-embedded embryos. Cell tracking analysis was performed using Imaris 8.2 (Bitplane).

### **Statistics**

All error bars indicate S.E.M. All p values were calculated with two-tailed statistical tests and 95% confidence intervals. Statistical tests were performed in Prism5 (GraphPad).

## Results and Discussion

A recent study showed that fusions of VSVG, a model membrane protein, with tandems of UVR8 spontaneously form clusters in the ER that are unable to traffic to the Golgi<sup>10</sup>. Upon UV exposure some of the clustered molecules are released and traffic to the plasma membrane within minutes<sup>10</sup>. This is evident immediately after activation as a more diffuse and extensive intracellular distribution<sup>10</sup>. It remains unclear whether UVR8 can be used for control of secreted proteins and for functional studies of any kind. We thus sought to establish a strategy tailored to signalling effectors secreted in the extracellular milieu by exploiting the light-responsive properties of UVR8 domains. We reasoned that a simple fusion of a secreted effector ligand with UVR8, as applied so far for control of membrane protein traffic<sup>10</sup>, might encounter at least three complications: i) photoactivation of UVR8 might not be as effective in the ER lumen as in the cytoplasm, which is the natural site of UVR8 activation<sup>11</sup>, ii) the large size of UVR8 could potentially interfere with biological activity and extracellular diffusion and presentation, iii) the possible re-oligomerisation of UVR8 in the extracellular environment cannot be easily measured and excluded *in vivo*. To prevent these complications, we exploited the fact that many secreted effectors, including hormones and growth factors, are naturally processed into their active form by furin, a Golgi-resident enzyme<sup>12</sup>. We engineered constructs so that the target, secreted protein is fused to the N-terminal, luminal part of a type I membrane protein (VSVG-ts045) with a consensus furin recognition sequence between the target secreted protein and the 'carrier' transmembrane protein (**Figure 1**). The C-terminal, cytoplasmic part of this construct contains 2 UVR8 tandems (**Figure 1**). As furin is resident in the Golgi<sup>12</sup>, molecules trafficking to the Golgi after photoactivation should be cleaved, leading to photo-dependent release of the target protein in the extracellular medium without the

UVR8 moiety (**Figure 1**). Thus, this strategy would maintain UVR8 in the cytoplasm and prevent any effects of UVR8 on extracellular protein activity and presentation, ensuring applicability to versatile ligands without special customizations.

We first tested this approach in HEK293T cells using a model, secreted mCherry (mCherry with a chemokine signal sequence<sup>13</sup>) as target ligand and YFP as a fluorescent reporter for the UVR8 moiety (**Supplementary figure 1A**). A short pulse of UVB light led to a redistribution of mCherry, along with YFP (**Supplementary figure 1B**). Redistribution was similar in a construct that did not carry the furin-recognition site confirming that there is no obvious leakiness of furin processing that could lead to mCherry mislocalisation (**Supplementary figure 1B**). Importantly, redistribution of mCherry-YFP-2xUVR8 (with the furin recognition site) was accompanied by release of mCherry in HEK293T cell supernatants (**Supplementary figure 1C and D**). In contrast, mCherry was not detectable in supernatants from cells that were not exposed to UV light or that expressed a construct lacking the furin cleavage site (**Supplementary figure 1C and D**), confirming the photo-dependent and furin-dependent control of mCherry secretion.

Next we tested this approach with a chemokine. We replaced secreted mCherry with mouse Cxcl2, the murine homologue of human CXCL8 (or IL-8), a well-characterized neutrophil attractant (**Figure 2A**). While the chemokine is not directly visible, the cytoplasmic YFP can be used as readout for successful photo-activation, a highly useful feature of this system (**Figure 2B**). Using different doses of UV light, we found that a minimum dose of 6 mJ could lead to significant release of the chemokine in the supernatant (**Figure 2C and D**). Consistent with previous reports<sup>10</sup>, we found that the minimum dose of UV required for UVR8 activation does not cause detectable cell toxicity (**Supplementary Figure 2**). Notably we detected two specific bands for Cxcl2 in

western blots of cell culture supernatants (**Supplementary Figure E**). In agreement with other reports on chemokine glycosylation<sup>14</sup>, we found that the higher molecular weight band corresponded to a glycosylated form of Cxcl2, as the band could be eliminated after PNGase treatment (**Figure 2C**). We further quantified the kinetics of Cxcl2 secretion. To this end we collected cell supernatants in 30 min intervals after photoactivation to assess new chemokine secretion. We found that the majority of chemokine release occurs between 30-60 min post UV exposure and is in the order of 0.15 fg/cell (Figure 2 E and F).

To verify the functionality of the photo-released chemokine, we used concentrated culture supernatants from photo-activated cells in a transwell chemotaxis assay (**Figure 3A**). Supernatants from photo-activated cells were more attractive to neutrophils than supernatants from non-photoactivated Cxcl2-YFP-2xUVR8-expressing cells and this attractive potential could be blocked by anti-Cxcl2 blocking antibody, confirming that the photo-released chemokine is functional (**Figure 3B**). The strong effect shown for the antibody blocking reflects inhibition of both photo-released chemokine and background chemokine (from dead cells or leakiness in secretion) in the concentrated supernatants. Supernatants from cells expressing wild type, constitutive Cxcl2, were equally attractive to neutrophils with or without UV exposure, confirming that light exposure specifically affects UVR8-conditioned protein trafficking (**Figure 3B**).

Next we investigated whether short pulses of chemokine could affect neutrophil behaviour. We co-cultured HEK293T cells expressing Cxcl2-YFP-2xUVR8 with primary mouse neutrophils and exposed the cells to UV (**Figure 4A**). We titrated the dose of UV to minimize any potential effects on neutrophil motility. We found that a single pulse of UV was sufficient to substantially increase the frequency of interactions between neutrophils and Cxcl2-YFP-2xUVR8 expressing cells (**Figure 4B-C** and **Movie 1**). In

contrast, UV exposure did not affect the frequency of interactions with mock-transfected cells (**Figure 4B**).

Finally we evaluated the potential to photo-activate chemokine secretion in a tissue context. We seeded mock or Cxcl2-YFP-2xUVR8-transfected HEK293T cells in surgically exposed ear dermis from BALB/c LysM-EGFP mice<sup>15</sup>, in which endogenous neutrophils express GFP (**Figure 5A**). Consistent with our in vitro evidence, we found that a single pulse of UV light led to an immediate change in Cxcl2-YFP-2xUVR8 distribution from perinuclear aggregates to diffuse intracellular distribution (**Figure 5B**) and a subsequent (within 30 minutes) increase in the number of contacts between transplanted cells and endogenous neutrophils (**Figure 5C-D** and **Movie 2**). A UV-light pulse on mock transfected HEK293T cells did not alter neutrophil behaviour confirming that the effect was dependent on the photo-released chemokine (**Figure 5D**). To further validate the in vivo applicability of our approach we performed analogous experiments in zebrafish with the corresponding chemokine homologue (zebrafish Cxcl8<sup>13</sup>). We locally injected zCxcl8-YFP-UVR8-transfected cells into Tg(*mpx*:Lifeact-Ruby) or Tg(*lyz*:DsRed) zebrafish embryos, in which neutrophils express a red fluorescent actin polymerization probe<sup>16</sup> or DsRed respectively, and imaged neutrophil behaviour one-day post transplantation (**Figure 5E**). Exposure of the larvae to a short pulse of UV light led to quick redistribution of zCxcl8-YFP-2xUVR8 (**Figure 5F**) and a marked increase (within 30 minutes) in the frequency of interactions between neutrophils and transplanted cells and a significant increase in the duration of contacts (**Figure 5G-H**, **Supplementary Figure 3A** and **Movie 3**), that was not seen in mock transfected control experiments (**Figure 5H** and **Movie 4**). Motility levels were not grossly affected by the photo-released chemokine, however we observed a significant increase in the path straightness of the cells, suggestive of more directed migration (**Supplementary Figure 3B and C**). The

level of neutrophil accumulation at the site of zCxc18 release was comparable to that observed with constitutively secreted zCxc18 by the same type of cellular source<sup>13</sup>, suggesting that gradient formation can be established immediately after secretion and does not require large amounts of ligand to be functional. Thus, photo-activation of UVR8 and manipulation of chemokine function can be achieved in an entirely non-invasive manner in organisms/tissue samples.

In summary, we present a new strategy to functionally control ligand secretion and cell communication by light *in vivo* that is widely applicable to a variety of signalling proteins including chemoattractants, cytokines, growth factors and morphogens. Several studies have shown that chemokines can enhance leukocyte contact dynamics<sup>17-19</sup>. We provide evidence that a short pulse of chemokine release is sufficient to alter the behaviour of neighbouring cells within minutes, suggesting that chemokine propagation and functional presentation can be established very rapidly *in vivo*. The ability to manipulate release of diffusible, signalling ligands *in vivo* in a pulsatile fashion should open new avenues for exploring how cells communicate during development, at steady-state or in the context of an immune response. Finally, our methodology may offer new possibilities in the context of immune cell therapies by offering spatiotemporal control for the release of desirable soluble effectors.

## **Acknowledgements**

We thank Matthew Kennedy for donation of the VSVG-2xUVR8 plasmid, Anna Huttenlocher for donation of the Tg(*mpx:Lifeact-Ruby*) transgenic line, Matthew Albert for access to the X97 UVB-BB (280-320 nm) UVB lamp source, Philippe Herbomel for access to an SP8 confocal microscope and H el ene Moreau for comments on the manuscript. This work was supported by Institut Pasteur, Inserm, the European Research Council (starting grant LymphocyteContacts to P.B.), and the Medical Research Council (RG73189 to M.S.).

## **Author contributions**

M.S. conceived the strategy. M.S., R.O and P.B. designed the research. M.S. and R.O. performed experiments and analyzed the data. M.S. and P.B. wrote the manuscript.

## **Conflict of Interest Disclosure**

The authors declare no competing financial interests



## References

1. Chen, X. *et al.* Chemical synthesis of a two-photon-activatable chemokine and photon-guided lymphocyte migration in vivo. *Nat. Commun.* 2015;6:7220.
2. Xu, Y. *et al.* Optogenetic control of chemokine receptor signal and T-cell migration. *Proc. Natl. Acad. Sci. U. S. A.* 2014;111(17):6371–6376.
3. Tischer, D. & Weiner, O. D. Illuminating cell signalling with optogenetic tools. *Nat. Rev. Mol. Cell Biol.* 2014;15(8):551–558.
4. Konermann, S. *et al.* Optical control of mammalian endogenous transcription and epigenetic states. *Nature* 2013;500(7463):472–476. doi:10.1038/nature12466
5. Ye, H., Baba, M. D.-E., Peng, R.-W. & Fussenegger, M. A Synthetic Optogenetic Transcription Device Enhances Blood-Glucose Homeostasis in Mice. *Science* 2011;332(6037):1565–1568.
6. Metzger, D., Clifford, J., Chiba, H. & Chambon, P. Conditional site-specific recombination in mammalian cells using a ligand-dependent chimeric Cre recombinase. *Proc. Natl. Acad. Sci. U. S. A.* 1995;92(15):6991–6995.
7. Bienz, M. & Pelham, H. R. Heat shock regulatory elements function as an inducible enhancer in the *Xenopus hsp70* gene and when linked to a heterologous promoter. *Cell* 1986;45(5):753–760.
8. Boncompain, G. *et al.* Synchronization of secretory protein traffic in populations of cells. *Nat. Methods* 2012;9(5):493–498.
9. Rivera, V. M. *et al.* Regulation of protein secretion through controlled aggregation in the endoplasmic reticulum. *Science* 2000;287(5454):826–830.
10. Chen, D., Gibson, E. S. & Kennedy, M. J. A light-triggered protein secretion system. *J. Cell Biol.* 2013;201(4):631–640.

11. Kaiserli, E. & Jenkins, G. I. UV-B promotes rapid nuclear translocation of the Arabidopsis UV-B specific signaling component UVR8 and activates its function in the nucleus. *Plant Cell* 2007;19(8):2662–2673.
12. Thomas, G. Furin at the cutting edge: from protein traffic to embryogenesis and disease. *Nat. Rev. Mol. Cell Biol.* 2002;3(10):753–766.
13. Sarris, M. *et al.* Inflammatory chemokines direct and restrict leukocyte migration within live tissues as glycan-bound gradients. *Curr. Biol.* 2012;22(24):2375–2382.
14. Ruggiero, P. *et al.* Glycosylation enhances functional stability of the chemotactic cytokine CCL2. *Eur. Cytokine Netw.* 2003;14(2):91–96.
15. Faust, N., Varas, F., Kelly, L. M., Heck, S. & Graf, T. Insertion of enhanced green fluorescent protein into the lysozyme gene creates mice with green fluorescent granulocytes and macrophages. *Blood* 2000;96(2):719–726.
16. Yoo, S. K. *et al.* Differential regulation of protrusion and polarity by PI3K during neutrophil motility in live zebrafish. *Dev. Cell* 2010;18(2):226–236.
17. Castellino, F. *et al.* Chemokines enhance immunity by guiding naive CD8<sup>+</sup> T cells to sites of CD4<sup>+</sup> T cell-dendritic cell interaction. *Nature* 2006;440(7086):890–895.
18. Friedman, R. S., Jacobelli, J. & Krummel, M. F. Surface-bound chemokines capture and prime T cells for synapse formation. *Nat. Immunol.* 2006;7(10):1101–1108.
19. Hickman, H. D. *et al.* CXCR3 chemokine receptor enables local CD8<sup>(+)</sup> T cell migration for the destruction of virus-infected cells. *Immunity* 2015;42(3):524–537.
20. Schaefer, B. C., Schaefer, M. L., Kappler, J. W., Marrack, P. & Kedl, R. M. Observation of antigen-dependent CD8<sup>+</sup> T-cell/ dendritic cell interactions in vivo. *Cell. Immunol.* 2001;214(2):110–122.
21. Muzumdar, M. D., Tasic, B., Miyamichi, K., Li, L. & Luo, L. A global double-fluorescent Cre reporter mouse. *Genesis* 2007;45(9):593–605.

## Figure Legends

### Figure 1. Strategy for optogenetic control of ligand secretion

A) Strategy for optogenetic triggering of ligand secretion. The target ligand is fused to the luminal side of a transmembrane protein (VSVG-ts045) and YFP and 2xUVR8 repeats on the cytoplasmic side. Before photoactivation (no PA), the construct forms clusters in the ER, with minimal trafficking to the Golgi. After photo-activation by UVB (PA), some fusion proteins get released and traffic to the Golgi whereby the target ligand is cleaved off by furin, leading to secretion of the desirable moiety in the extracellular medium. B) Representation of cells in tissue before and after photoactivation. Target ligand gradient is shown in red.

### Figure 2. Optogenetic control of chemokine secretion.

A) Construct design for optogenetic triggering of murine Cxcl2. B) Distribution of Cxcl2-YFP-2xUVR8 before or after photoactivation (PA) with 9 mJ. Scale bar=20µm. C) Detection of cleaved Cxcl2 in supernatants and uncleaved Cxcl2-YFP-2xUVR8 in lysates from non-treated (no PA) or photo-activated cells with indicated doses of UVB. Supernatant samples were treated with PNGase in order to obtain single bands representing non-glycosylated chemokine. D) Quantification of protein in the supernatant samples shown in C, based on band intensity normalized against the lysate bands and relative to the 'no PA' condition. E) Time course of cleaved Cxcl2 secretion. Supernatants were collected in 30-min intervals, washing the cells in between collection time points, to assess new chemokine production. F) Quantification of exact protein amount shown in E.

**Figure 3. Photo-released chemokine is functional.**

A) Evaluation of functionality of photo-released chemokine in a transwell chemotaxis assay. The bottom chamber was loaded with supernatants from cells transfected with a mock plasmid or Cxcl2-YFP-2xUVR8 or constitutive Cxcl2 and then photo-activated or not. Freshly isolated mouse neutrophils were placed in the top chamber. B) Number of neutrophils transmigrated over background migration (determined by migration to mock supernatants). Data points represent multiple wells within one experiment representative of four independent experiments. Unpaired t test was applied.

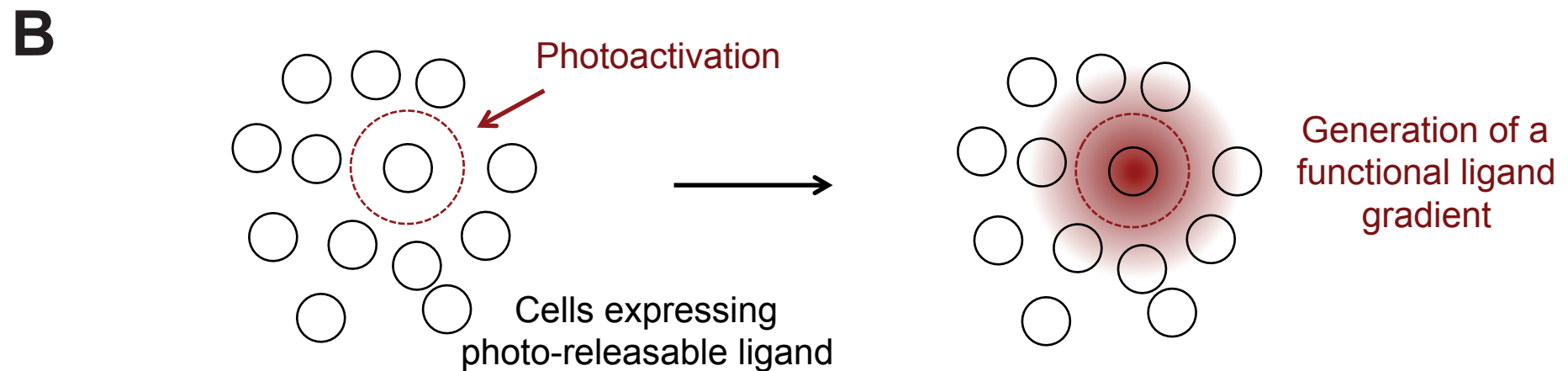
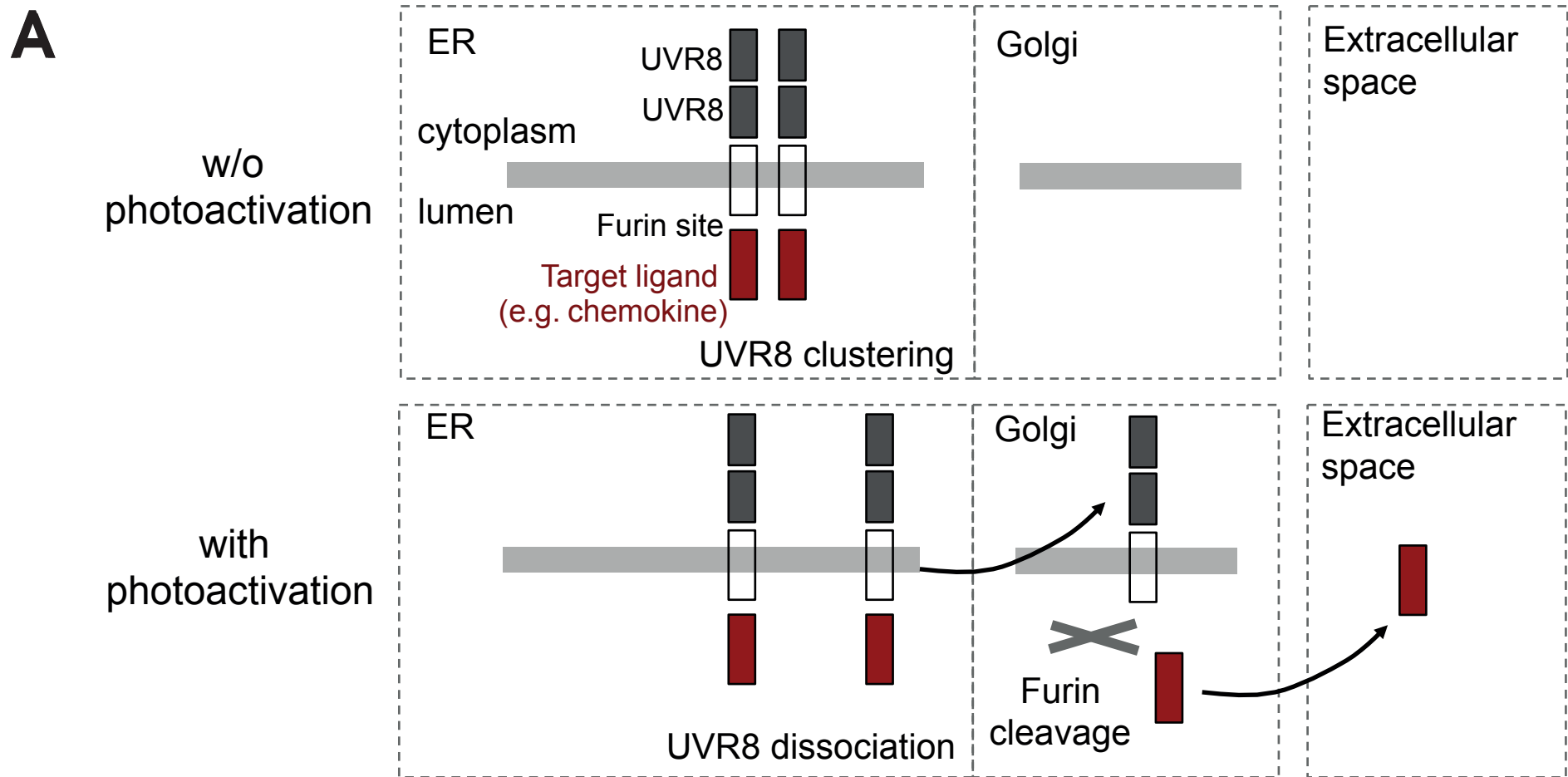
**Figure 4. A brief, light-triggered pulse of chemokine secretion rapidly enhances cell interactions *in vitro*.**

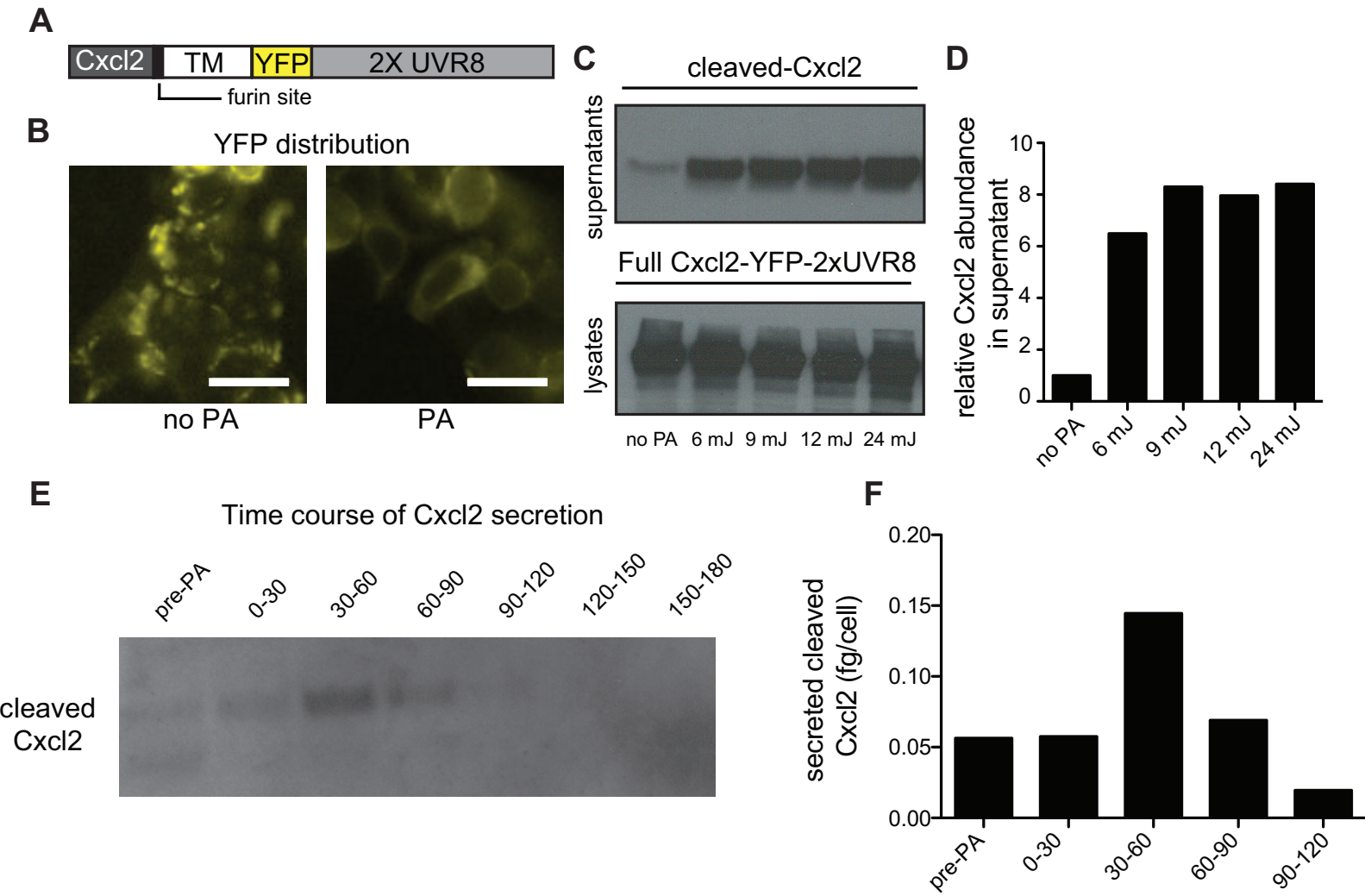
A) Representative images of co-cultured HEK293T cells and mouse neutrophils before and after activation. White arrows indicate contacts. Scale bar=25µm. B) Percentage of neutrophils forming contacts with transfected HEK293T cells (out of the number of neutrophils present in the same area). Repeated measures ANOVA with Bonferroni post-test was applied. n=3 values representing independent experiments. Error bars represent S.E.M. C) Examples of contact formation after photoactivation of Cxcl2 secretion. Scale bar=10µm.

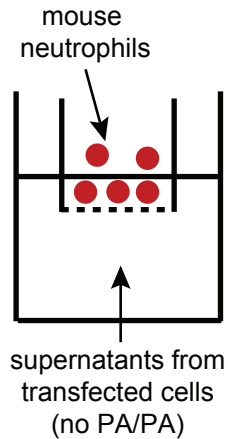
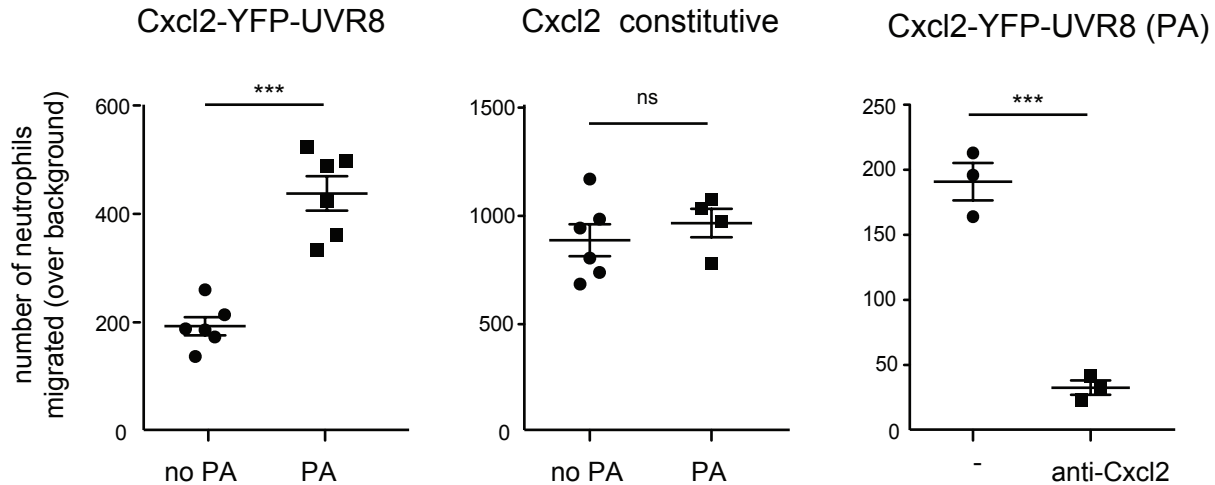
**Figure 5. A brief, light-triggered pulse of chemokine secretion rapidly enhances cell interactions *in vivo* in mouse tissue and in zebrafish.**

A) Experimental scheme for optogenetic control of chemokine release in mouse tissue. The ear dermis from an anaesthetized LysM-GFP mouse was surgically exposed and seeded with HEK293T cells expressing Cxcl2-YFP-2xUVR8. B) Distribution of Cxcl2-YFP-2xUVR8 before and after photoactivation (PA). C) Representative images of ear

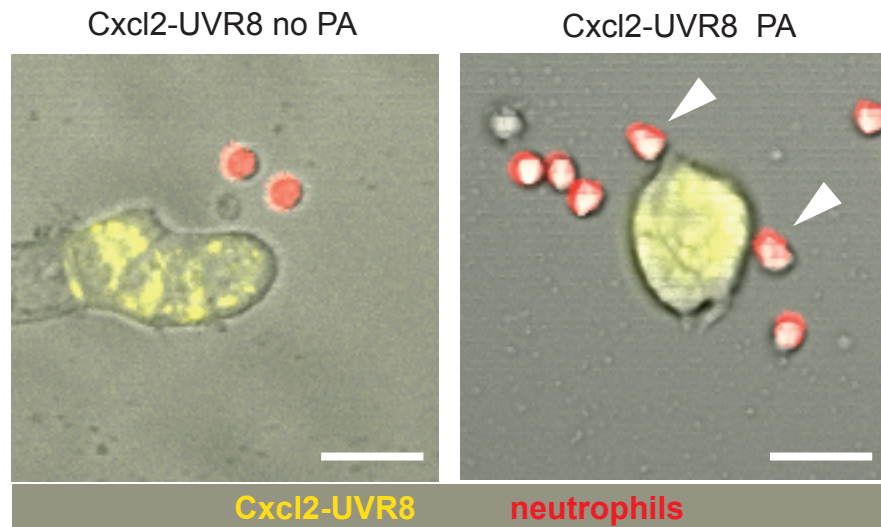
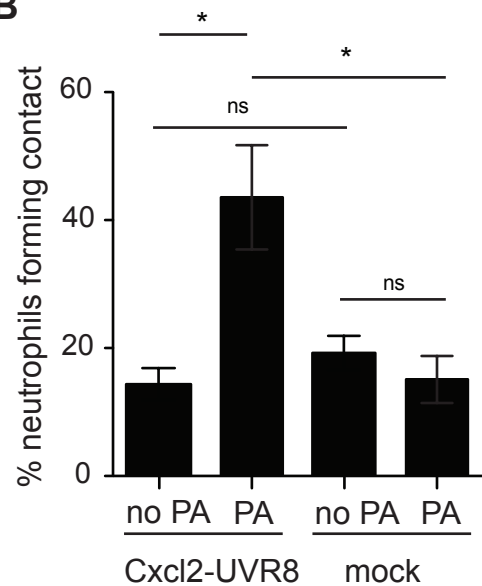
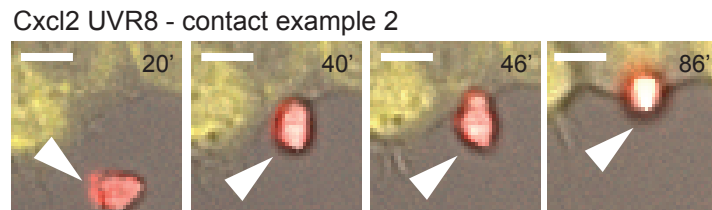
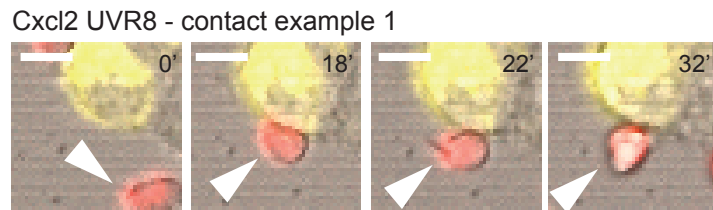
tissue with mouse neutrophils (red) and HEK293T cells (yellow). Arrows indicate contacts between the cells. D) Number of contacts formed between individual HEK293T cells and neutrophils before and after PA, normalized to number of neutrophils in the field and relative to no PA condition (n=63 Cxcl2-YFP-2xUVR8-transfected and n=48 mock GFP-transfected HEK293T cells, pooled data from 2-4 250 x 250  $\mu\text{m}$  regions of interest per mouse and at least 3 mice per experimental condition, paired t test). E) Experimental scheme for optogenetic control of chemokine release in zebrafish. Mock or zebrafish Cxcl8-YFP-UVR8-transfected HEK293T cells were locally transplanted in transgenic *mpx:Lifeact-Ruby* zebrafish larvae and mounted for imaging and photoactivation. F) Distribution of Cxcl8-YFP-UVR8 before and after photoactivation (PA). G) Representative images of zebrafish neutrophils (red) in the area of HEK293T cell implantation (yellow). H) Number of contacts formed between individual HEK293T cells and neutrophils before and after PA, normalized to number of neutrophils in the field and relative to no PA condition (n=43 Cxcl8-YFP-UVR8-transfected and n=18 mock GFP-transfected HEK293T cells, pooled data from 3 larvae in 2 independent experiments, paired t test). Error bars represent S.E.M. Scale bar=25  $\mu\text{m}$  in all images.

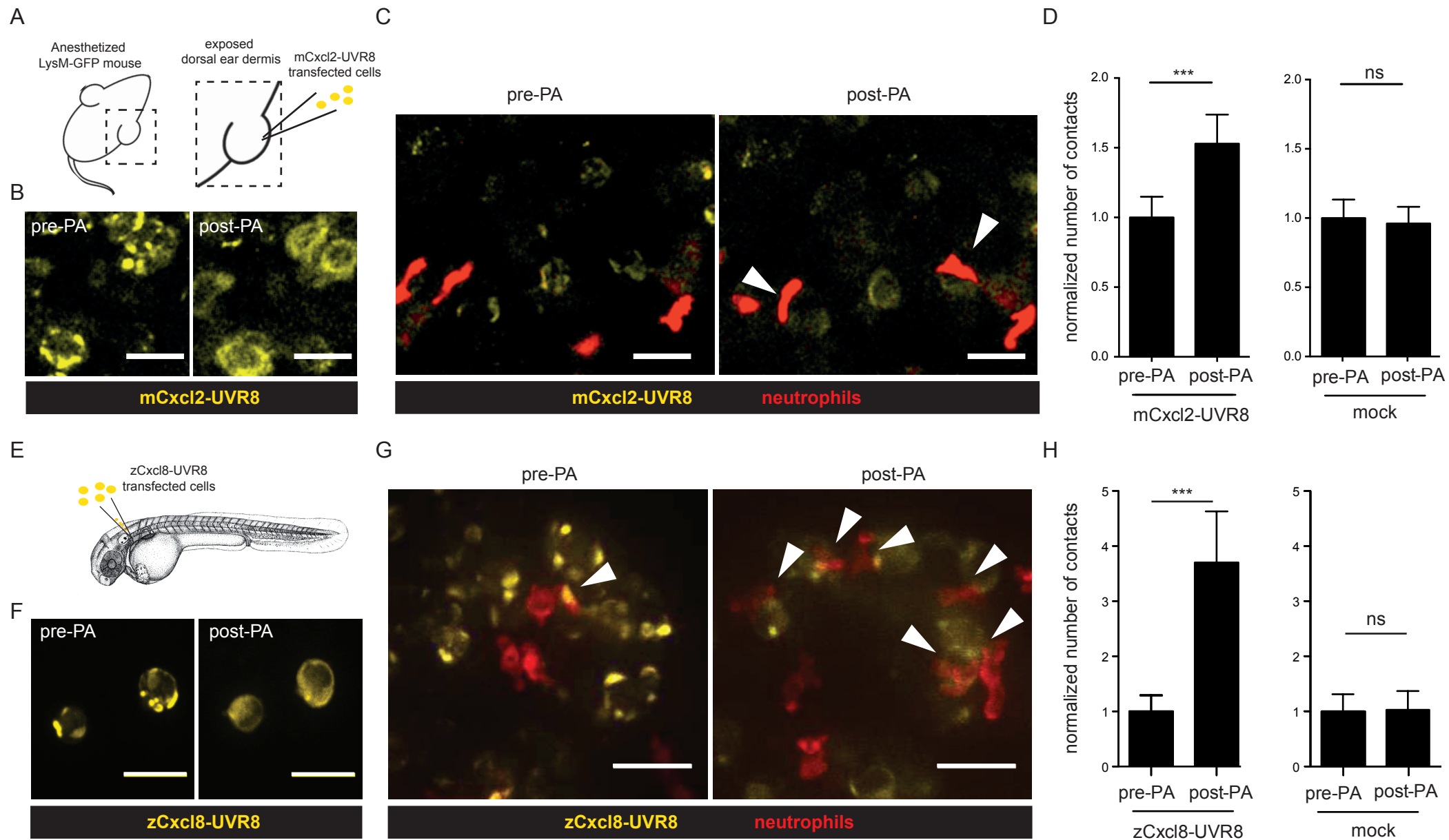




**A****B**



**A****B****C**





**blood**<sup>®</sup>

Prepublished online April 7, 2016;  
doi:10.1182/blood-2015-11-684852

## **Manipulating leukocyte interactions in vivo through optogenetic chemokine release**

Milka Sarris, Romain Olekhovitch and Philippe Bousso

---

Information about reproducing this article in parts or in its entirety may be found online at:  
[http://www.bloodjournal.org/site/misc/rights.xhtml#repub\\_requests](http://www.bloodjournal.org/site/misc/rights.xhtml#repub_requests)

Information about ordering reprints may be found online at:  
<http://www.bloodjournal.org/site/misc/rights.xhtml#reprints>

Information about subscriptions and ASH membership may be found online at:  
<http://www.bloodjournal.org/site/subscriptions/index.xhtml>

---

Advance online articles have been peer reviewed and accepted for publication but have not yet appeared in the paper journal (edited, typeset versions may be posted when available prior to final publication). Advance online articles are citable and establish publication priority; they are indexed by PubMed from initial publication. Citations to Advance online articles must include digital object identifier (DOIs) and date of initial publication.